POAC'17
Busan, KOREA

Proceedings of the 24th International Conference on
Port and Ocean Engineering under Arctic Conditions
June 11-16, 2017, Busan, Korea

A Three-Dimensional FEM-DEM Model of an Ice Sheet

Ville-Pekka Lilja[1], Arttu Polojärvi[1], Jukka Tuhkuri[1], Jani Paavilainen[2]
[1] Aalto University, School of Engineering, Department of Mechanical Engineering, Finland
[2] Rand Simulation Ltd., Vantaa, Finland

ABSTRACT

A three-dimensional combined finite-discrete element (FEM-DEM) model of an ice sheet is presented. Centroidal Voronoi tessellation with a random generating point set is used to produce an unstructured mesh. Mesh consists of convex polyhedra as the discrete elements and a Delaunay-triangulated network, or a lattice, of Timoshenko beam elements connecting their mass centroids. We investigate, by performing simple in-plane and out-of-plane mechanical tests, how the model behaves while the sheet is still intact. We compute the effective Young's modulus and study the bending of an ice sheet on an elastic foundation for several different specimen sizes.

KEY WORDS: Ice; Combined FEM-DEM; Beam lattice network; Size effect; Bending

INTRODUCTION

A sea ice sheet interacting with a structure deforms and eventually breaks into a large number of distinct fragments. Broken fragments accumulate in front of the structure and affect the subsequent failure process. Modeling the interaction process is computationally demanding and requires the development of efficient methods.

This paper presents a three-dimensional combined finite-discrete element (FEM-DEM) model of an ice sheet meant to be used for conducting such ice-structure interaction simulations. We investigate, by performing simple in-plane and out-of-plane mechanical tests, how the model behaves while the sheet is still intact. We compute the effective Young's modulus and study the bending of an ice sheet on an elastic foundation for several different specimen sizes.

Similar, namely discrete element, combined finite-discrete element, finite element, or lattice-based numerical methods to model a floating ice sheet and its interaction with an offshore structure have been used in the past by for example Hocking (1992), Jirásek & Bažant (1995), Hopkins (1998), Sayed & Timco (1998), Selvadurai & Sepehr (1999), Sand (2008), Dorival et al. (2008), Konuk et al. (2009), Gürtner (2009), Paavilainen (2013), Kuutti et al. (2013), Lu et al. (2014), Herman (2016) and van den Berg (2016).

CONSTRUCTION OF THE NUMERICAL MODEL

The modeled ice sheet consists of a network of two-noded, three-dimensional, co-rotational Timoshenko beam elements connected with the mass centroids of the overlaid undeformable discrete elements, Figure 1. Centroidal Voronoi tessellation (CVT) with a random generating point set and Lloyd's algorithm, (Du et al., 1999), is used to produce an unstructured mesh, Figure 2. Mesh consists of convex polyhedra as the discrete elements and a Delaunay-triangulated network, or a lattice, of Timoshenko beam elements.

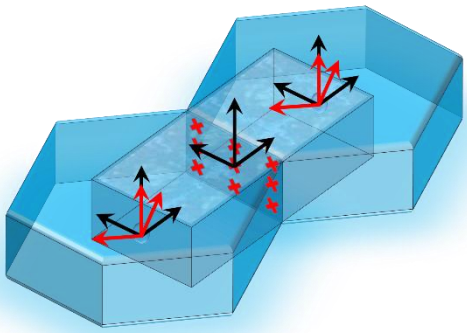

Figure 1. Two discrete elements connected with a Timoshenko beam element.

Elasticity of an ice sheet, prior to fracture, is modeled solely with the beams, contacts between the broken pieces of ice by the discrete elements. The beam formulation follows closely Crisfield (1990,1997) while the contacts between the discrete elements are resolved as in Polojärvi et al. (2012). For the beams, Hooke's linearly elastic constitutive law, with a viscous damping model, is used. To model damage, the beams are allowed to fracture allowing a crack to propagate along an interface separating two adjacent discrete elements. This paper does not, however, consider fracture. For a description of fracture, see Lilja et al. (2017). In esse nce, the model is a three-dimensional extension of our earlier two-dimensional FEM-DEM model by Paavilainen et al. (2009) and was introduced by Paavilainen (2010).

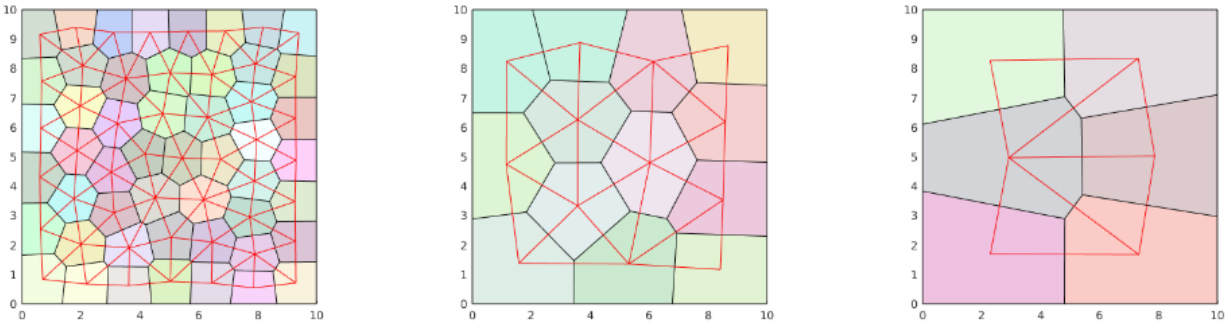

Figure 2. Three CVT-tessellated square-shaped ice sheets with a side length of L = 10 m. From left to right, sheets having a thickness of h = 0.5, 1.0 and 1.5 m and a discrete element size of $l = 3h$. Cross-sectional area of each beam element gets determined by the area of the joint surface separating two adjacent discrete elements. Red lines denote the longitudinal axes of the beam elements.

A sea ice sheet modeled as described above behaves mechanically as a cellular solid. Effective macroscopic material properties behave as functions of the ratio between the macroscopic size of an ice sheet and the size of a unit cell of the beam lattice network in use: there is a size effect. It can be also shown that a beam element network is a discrete equivalent of a micropolar continuum (Bažant & Christensen, 1972), and that on a large enough scale a CVT-tessellated mesh behaves like a transversely isotropic medium, as the mesh consists of beams forming (nearly) equilateral triangles.

Equations to be solved for each discrete element, discretely in time, are the three translational equations of motion and the three rotational equations of motion. Internal forces and moments inside a sheet consist of the resultants of all the nodal force and moment components of all the deformable beam elements sharing nodes with the discrete elements. Simulations are explicit.

SIMULATIONS

Main goals of our simulations are: (1) to compute the effective Young's modulus E of an ice sheet for several different specimen sizes and (2) to test how well our model describes a floating ice sheet in bending. Values of the computed effective Young's moduli E are compared with the Young's modulus E^{b} as given to the beams and with the Young's modulus E^{*} of an infinite lattice composed of Timoshenko beams and having a regular topology consisting of perfectly hexagonal unit cells (beams forming equilateral triangles) using the theory of a micropolar continuum (Ostoja-Starzewski, 2002; Karihaloo et al., 2003). Bending of an elastic ice sheet on an elastic foundation having a concentrated vertical point load is investigated subsequently. Deflections are compared with the deflections of a point-loaded infinite ice sheet floating on water, as presented by Wyman (1950).

Mesh Creation

Figure 3 shows the sheets used in the tests. Sheets were square-shaped and had the side lengths of L = 10, 20, 40, 80 and 160 m and the thicknesses of h = 0.5, 1.0 and 1.5 m. For each sheet, we used two mesh densities: a mesh with an average discrete element size of $l = 2h$ and a mesh with an average discrete element size of $l = 3h$. In the case of a possible fracture, each broken fragment should have, thus, in minimum, a size that is comparable with actual block sizes measured from ridge sails (Kankaanpää, 1988; Høyland, 2007; Kulyakhtin, 2014). Ten randomized CVT-meshes were created for all of the sheets, excluding the sheet with L=160 m, h = 0.5 m and $l = 2h$, for which six meshes were produced.

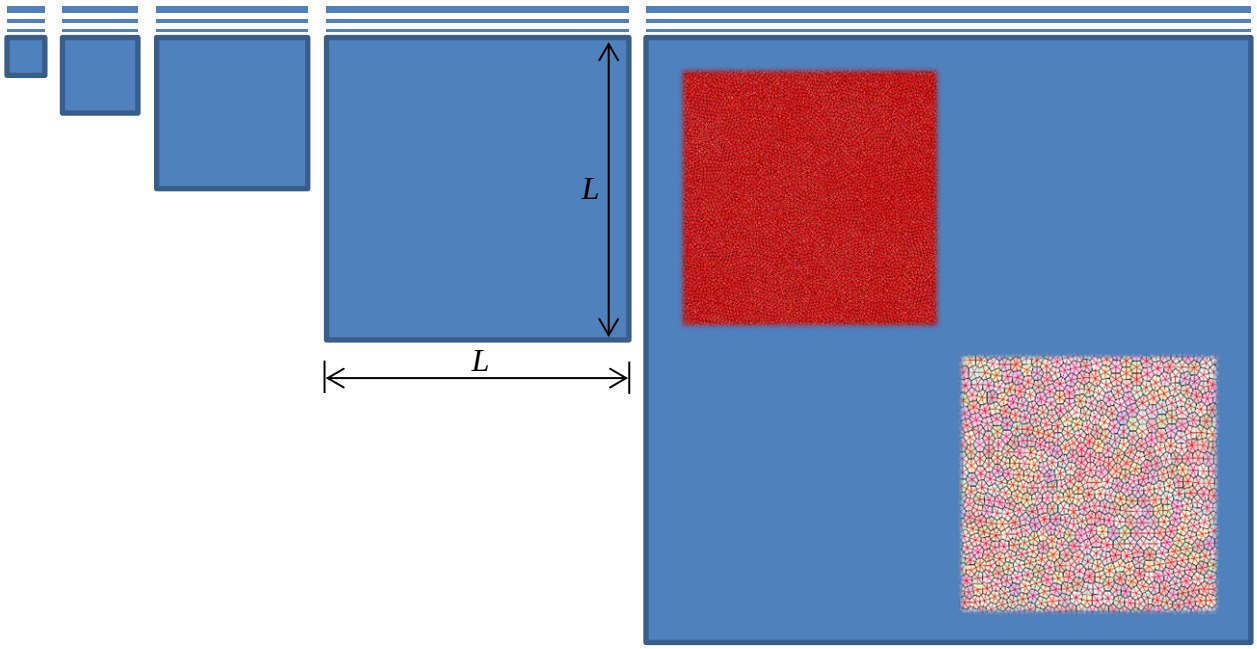

Figure 3. Size range (1:16) of the ice sheets considered. From left to right: L = 10, 20, 40, 80 and 160 m. The largest sheet on the right shows also sections of the two meshes that have the most and the least amount of discrete elements for that size: 29561 discrete elements (h = 0.5 m, l = 2h) and 1460 discrete elements (h = 1.5 m, l = 3h).

Effective Young's Modulus

Effective Young's modulus E was computed by carrying out a simple uniaxial tensile test. Each sheet was loaded under displacement control, as shown in Figure 4. Nodes on the right boundary were pulled with a constant velocity v = 0.1 m/s into the positive X-direction while the X-direction motion of the nodes on the left boundary were fixed. There were no other constraints in the system. Beams were not allowed to fracture.

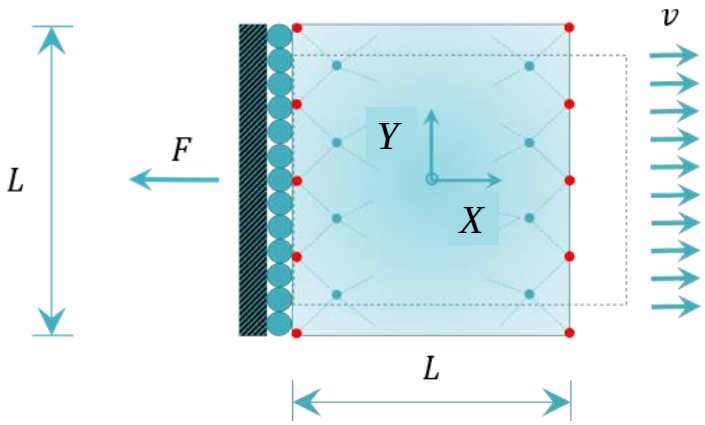

Figure 4. Boundary conditions and the reaction force F used in the computation of the effective Young's modulus E.

Effective Young's modulus E was evaluated through Hooke's law as $E = F/(A_0\varepsilon_X)$, where F is the computed resultant boundary reaction, $A_0 = Lh$ is the initial cross-sectional area of an ice sheet and ε_X is the applied axial strain (a value of 0.001 was used). Reaction F was calculated for each sheet by summing up the X-direction components of the internal nodal force vectors of the beams having nodes on the left boundary. Table 1 shows the main parameters of the simulations.

Table 1. Main simulation parameters.

Parameter	Symbol	Unit	Value
Young's modulus	E^b	GPa	4
Poisson's coefficient	ν		0.3
Density of ice	ρ_{ice}	kg/m^3	920
Density of water	ρ_{water}	kg/m^3	1010
Damping constant	c		critical[1]
Time step	Δt	s	$1.0\times10^{-5}\ldots5.0\times10^{-5}$
Acceleration of gravity	g	m/s^2	9.81

[1] $c = \sqrt{m_{eff}E^b}$, where m_{eff} is the average of the masses of the two discrete elements a beam connects.

Results

Figure 5 shows the computed effective average Young's moduli E and their standard deviations as functions of sheet size L, sheet thickness h and discrete element size l. Results shown are the averages calculated using ten randomized CVT-meshes, except for the case with L=160 m, h = 0.5 m and $l = 2h$, for which six meshes were used. For each L the results are arranged in an order of ascending h and l (for each h). Modulus E grows as a function of h and decreases as a function of L. For the smallest sheet size the differences between the results, whether a discrete element size of either $l = 2h$ or $l = 3h$ is used, are large. Sheets that are smaller, thicker or meshed with a discrete element size of $l = 3h$ have a higher E.

Figure 6 shows the ratios E/E^* and E/E^b as functions of the relative sheet size $L_{rel} = L/l$. The upper curve corresponds to the ratios E/E^* between the effective and the micropolar Young's moduli and the lower curve to the ratios E/E^b between the effective and the material (as given to the beams) Young's moduli. Ratio E/E^* converges approximately to a value of 1.0. Ratio varies from approximately 1.94 for the smallest and the thickest sheets to approximately 1.0 for the largest sheets. Ratio E/E^b converges approximately to a value of 0.8. Ratio varies from approximately 1.53 for the smallest and the thickest sheets to approximately 0.8 for the largest sheets. Size effect vanishes (practically) for $L_{rel} \geq 25$. Except for the smallest and the thickest sheets, having only a few elements across a sheet, deviations are observed to be small.

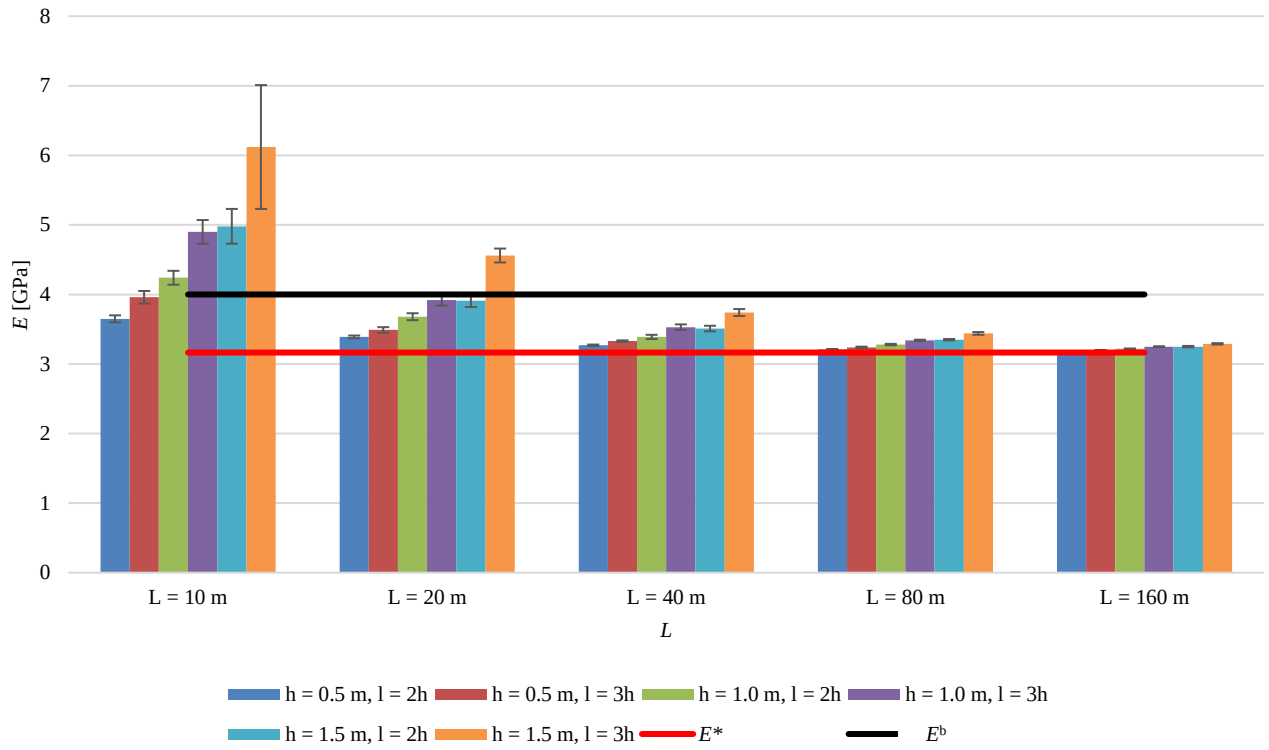

Figure 5. Effective Young's modulus E as a function of sheet size L, sheet thickness h and discrete element size l. Young's modulus E^b of the beams is indicated with a black color and the Young's modulus E^* as predicted by using the theory of a micropolar continuum with a red color.

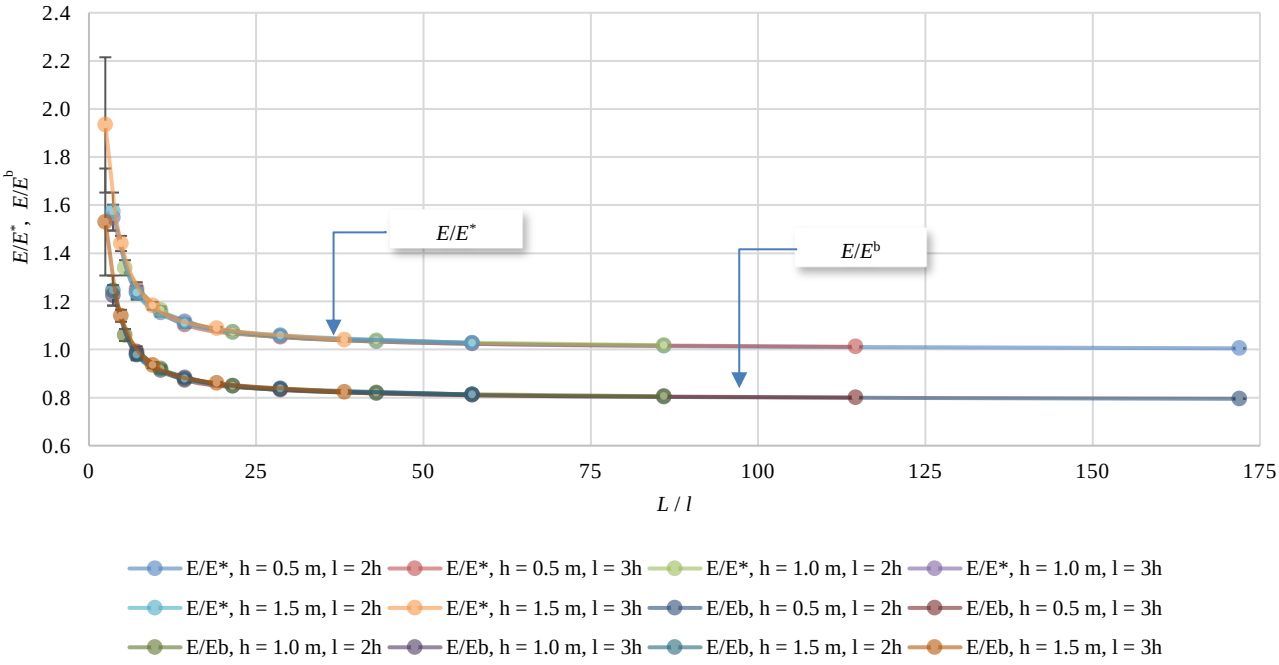

Figure 6. Ratios E/E^* and E/E^b as functions of the relative sheet size $L_{rel} = L / l$.

Bending of an Ice Sheet

Bending tests were done on an elastic foundation modeled by using both buoyancy and drag. Stoke's drag (a drag model giving a drag force that is linearly proportional to the absolute velocity) was used to reach a quasi-static equilibrium. A vertical point load $F_Z = -10$ kN (acting towards water, see Figure 4) was applied to a node that was closest to the geometrical center of each sheet by using a statically equivalent force system. Deflections were measured along a path: $X = 0$, $0 \leq Y \leq L/2$, corresponding to the edge of a quadrant of each sheet. Gravitation was taken into account, no displacement constraints were applied, beams were not allowed to fracture and the smallest sheets were excluded from the analysis. Sheets did not submerge under the loading.

Results

Figure 7 shows the average deflection profiles (with their standard deviations) of all the sheet sizes as functions of their normalized half-widths. Deflection profiles represent the average deflection profiles calculated using ten randomized CVT-meshes (for the case with L = 160 m, h = 0.5 m, $l = 2h$, with six meshes). Deflections are normalized with the maximum deflection of an infinite ice sheet having a thickness h, loaded by a concentrated vertical point load F_Z and floating on water (Wyman, 1950). Deflection profiles of the L = 80 m and the L = 160 m sheets are shown, again, in Figure 8.

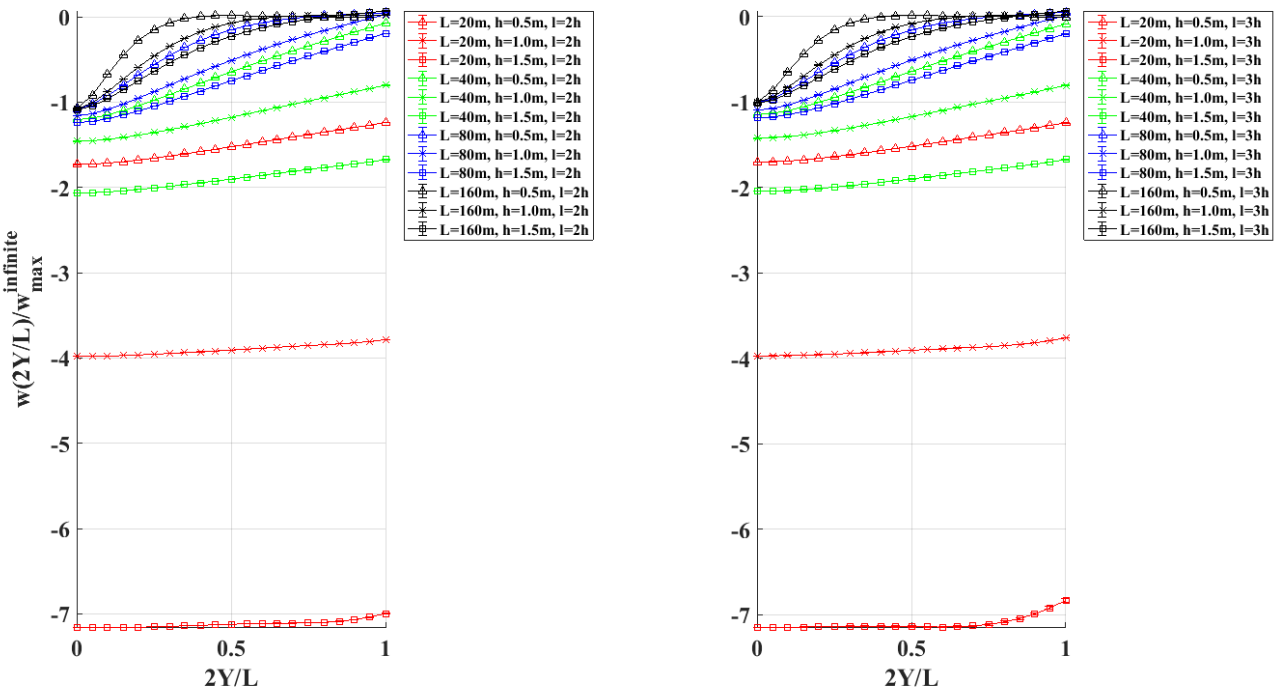

Figure 7. Normalized deflection profiles of all the sheet sizes as functions of their normalized half-widths. Discrete element size on the left: $l = 2h$, discrete element size on the right: $l = 3h$.

As the sheet size grows, the maximum deflections approach those by Wyman (1950). As the sheets get smaller or thicker, sheets tend to deform less and sink. Differences between the deflection profiles, whether a discrete element size of either $l = 2h$ or $l = 3h$ is used, are small. The maximum deflections, however, agree slightly better with Wyman (1950) when a discrete element size of $l = 3h$ is used.

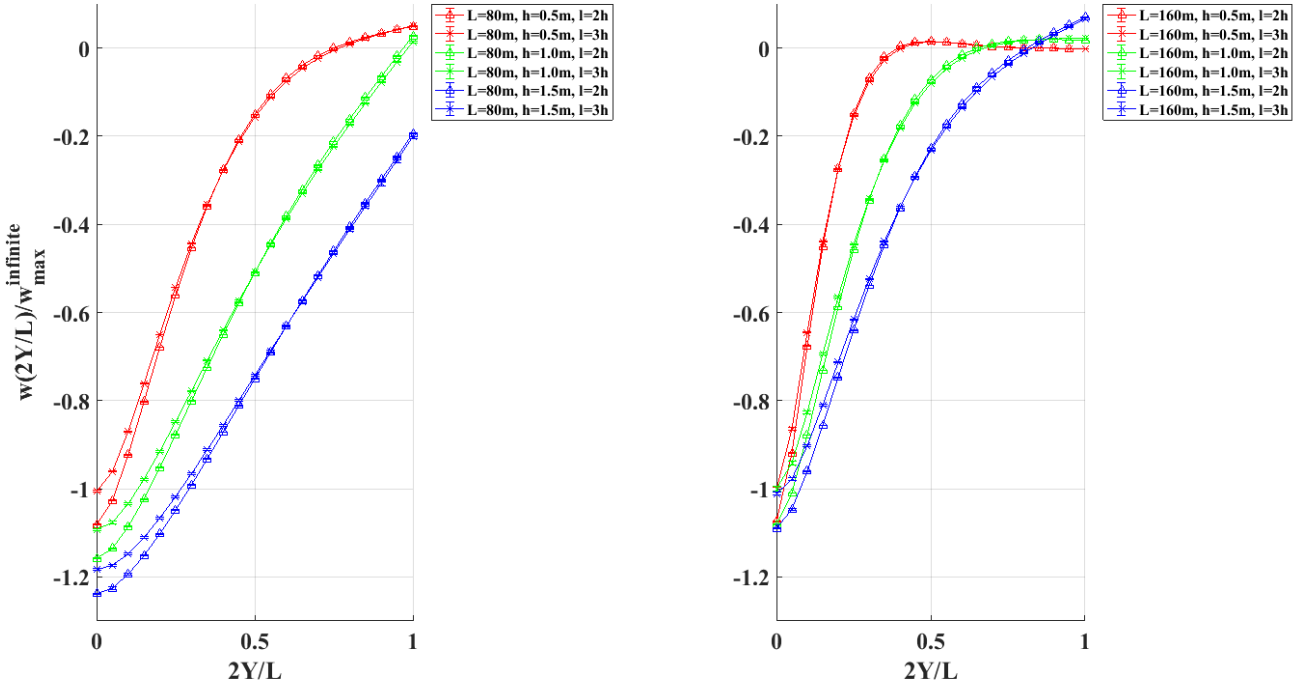

Figure 8. Normalized deflection profiles of the L = 80 m and the L = 160 m sheets as functions of their normalized half-widths.

Figure 9 shows the deflection profiles of the largest L = 160 m sheets as functions of characteristic length ($l_{ch} = \sqrt[4]{D/k}$, where $D = E^b h^3 / 12(1-\nu^2)$ is the flexural stiffness of an ice sheet and $k = \rho_{water} g$ is the specific weight of water). Deflections are, again, normalized with the maximum deflection of an infinite ice sheet having a thickness h, loaded by a concentrated vertical point load F_Z and floating on water (Wyman, 1950). Deflection of an infinite ice sheet is shown with a dashed line.

Deflections follow the corresponding normalized analytical deflection profiles well, especially for the two thinnest sheets. They, thus, seem to be able to represent point-loaded infinite ice sheets floating on water (with corresponding thicknesses) fairly well.

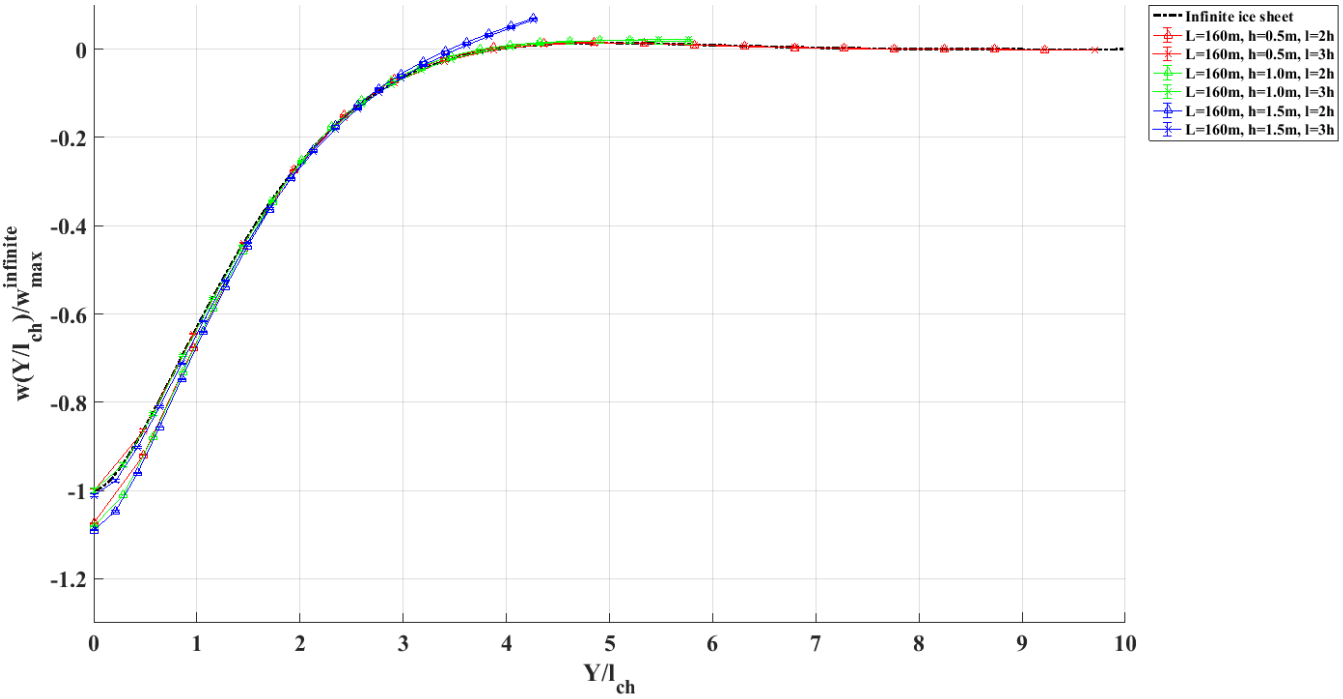

Figure 9. Normalized deflection profiles of the largest L = 160 m sheets as well as the analytical deflection profile of an infinite ice sheet loaded by a concentrated vertical point load and floating on water (Wyman, 1950).

CONCLUSIONS

A three-dimensional FEM-DEM model of an ice sheet was presented. Model consists of rigid discrete elements joined by two-noded, three-dimensional, co-rotational Timoshenko beam elements. Centroidal Voronoi tessellation was used to create the meshes.

Effective Young's modulus E was computed as a function of sheet size L, sheet thickness h and discrete element size l by carrying out a simple uniaxial tensile test. Sheets that are smaller, thicker or have a coarser mesh have a higher effective Young's modulus E. Size effect vanishes (practically) for $L_{\mathrm{rel}} \geq 25$.

Ratio between the effective Young's modulus E and the Young's modulus E^* as calculated by using the theory of a micropolar continuum (using as a reference topology an infinite regular lattice composed of Timoshenko beams forming perfectly equilateral triangles) converges approximately to a value of 1.0. Ratio between the effective Young's modulus E and the Young's modulus E^{b} of the beams converges approximately to a value of 0.8.

Bending of an elastic ice sheet on an elastic foundation was studied in the case of central loading. As the sheet size grows, the maximum deflections approach those by Wyman (1950). As the sheets get smaller or thicker, the sheets tend to deform less and sink. The sheets having a size of L = 160 m and the thicknesses of either h = 0.5 m or h = 1.0 m seem to be able to represent point-loaded infinite ice sheets floating on water (with the same thicknesses) fairly well.

ACKNOWLEDGEMENTS

Authors gratefully acknowledge the financial support by the Academy of Finland through the project: “Discrete Numerical Simulation and Statistical Analysis of the Failure Process of a Non-homogeneous Ice Sheet Against an Offshore Structure.”

REFERENCES

Bažant, Z. P. & Christensen, M., 1972. Analogy between micropolar continuum and grid frameworks under initial stress. *International Journal of Solids and Structures,* Volume 8, pp. 327-346.

Crisfield, M. A., 1990. A consistent co-rotational formulation for non-linear, three-dimensional, beam-elements. *Computer methods in applied mechanics and engineering,* Volume 81, pp. 131-150.

Crisfield, M. A., 1997. chs. 17.1-2. In: *Non-linear Finite Element Analysis of Solids and Structures, volume 2: Advanced Topics.* John Wiley & Sons Ltd.: New York, pp. 213-232.

Dorival, O., Metrikine, A. & Simone, A., 2008. *A lattice model to simulate ice-structure interaction.* ASME 2008 27th International Conference on Offshore Mechanics and Arctic Engineering, Estoril, Portugal, pp. 989-996.

Du, Q., Faber, V. & Gunzburger, M., 1999. Centroidal Voronoi Tessellations: Applications and Algorithms. *SIAM Review,* Volume 41, p. 637–676.

Gürtner, A., 2009. *Experimental and Numerical Investigations of Ice-Structure Interaction,* Doctoral thesis, Norwegian University of Science and Technology, NTNU: Trondheim.

Herman, A., 2016. Discrete-Element bonded-particle Sea Ice model DESIgn, version 1.3a – model description and implementation. *Geoscientific Model Development,* Volume 9, p. 1219–1241.

Hocking, G., 1992. The discrete element method for analysis of fragmentation of discontinua. *Engineering Computations,* Volume 9, pp. 145 - 155.

Hopkins, M., 1998. Four stages of pressure ridging. *Journal of geophysical research,* Volume 103, pp. 21883-21891.

Høyland, K. V., 2007. Morphology and small-scale strength of ridges in the North-Western Barents Sea. *Cold Regions Science and Technology,* Volume 48, pp. 169-187.

Jirásek, M. & Bažant, Z. P., 1995. Particle Model for Quasibrittle Fracture and Application to Sea Ice. *Journal of Engineering Mechanics,* Volume 121, pp. 1016-1025.

Kankaanpää, P., 1988. Morphology of sea ice pressure ridges in the Baltic Sea. *Geophysica,* Volume 24, pp. 15-44.

Karihaloo, B. L., Shao, P. F. & Xiao, Q. Z., 2003. Lattice modelling of the failure of particle composites. *Engineering fracture mechanics,* Volume 70, pp. 2385-2406.

Konuk, I., Gürtner, A. & Yu, S., 2009. *A Cohesive Element Framework for Dynamic Ice-Structure Interaction Problems - Part I: Review and Formulation.* ASME 2009 28th International Conference on Ocean, Offshore and Arctic Engineering, Honolulu, Hawaii, USA, May 31 - June 5, pp. 33-41.

Kulyakhtin, S., 2014. *Distribution of Ice Block Sizes in Sails of Pressure Ice Ridges.* 22nd IAHR International Symposium on Ice, Singapore, August 11 to 15.

Kuutti, J., Kolari, K. & Marjavaara, P., 2013. Simulation of ice crushing experiments with cohesive surface methodology. *Cold Regions Science and Technology*, Volume 92, pp. 17-28.

Lilja, V. P., Polojärvi, A., Tuhkuri, J. & Paavilainen, J., 2017. *Effective tensile strength of an ice sheet using a three-dimensional FEM-DEM approach.* Proceedings of the 24th International Conference on Port and Ocean Engineering under Arctic Conditions, Busan, Korea, June 11-16.

Lu, W., Lubbad, R. & Løset, S., 2014. Simulating Ice-Sloping Structure Interactions With the Cohesive Element Method. *Journal of Offshore Mechanics and Arctic Engineering,* Volume 136, pp. 1-16.

Ostoja-Starzewski, M., 2002. Lattice models in micromechanics. *Applied Mechanics Reviews,* Volume 55, pp. 35-60.

Paavilainen, J., 2010. Jäälautan murtuminen kartiorakennetta vasten. In: J. Heinonen, ed. *Jatkuvan murtumisprosessin mallinnus jää-rakenne vuorovaikutusprosessissa*, research report (in Finnish), project: "STRUTSI". Technical Research Center of Finland, Espoo: VTT, pp. 25-27.

Paavilainen, J., 2013. *Factors affecting ice loads during the rubbling process using a 2D FE-DE Approach*, Doctoral thesis, Aalto University: Espoo.

Paavilainen, J., Tuhkuri, J. & Polojärvi, A., 2009. 2D combined finite-discrete element method to model multi-fracture of beam structures. *Engineering computations,* Volume 26, pp. 578-598.

Polojärvi, A., Tuhkuri, J. & Korkalo, O., 2012. Comparison and analysis of experimental and virtual laboratory scale punch through tests. *Cold Regions Science and Technology*, Volume 81, pp. 11-25.

Sand, B., 2008. *Nonlinear finite element simulations of ice forces on offshore structures*, Doctoral thesis, Luleå University of Technology: Luleå.

Sayed, M. & Timco, G., 1998. *A Lattice Model of Ice Failure,* National Research Council of Canada: Ottawa.

Selvadurai, A. P. S. & Sepehr, K., 1999. Two-dimensional discrete element simulations of ice-structure interaction. *International Journal of Solids and Structures,* Volume 36, pp. 4919-4940.

van den Berg, M., 2016. *A 3-D Random Lattice Model of Sea Ice.* Arctic Technology Conference, St. John's, Newfoundland and Labrador, Canada, 24-26 October.

Wyman, M., 1950. Deflections of an infinite plate. *Canadian Journal of Research*, Volume 28, pp. 293-302.